

ARTICLE



Mild MDPL in a patient with a novel de novo missense variant in the Cys-B region of *POLD1*

Maya Chopra^{1,2}, Richard Caswell³, Giulia Barcia⁴, Sophie Rondeau⁴, Laurence Jonard^{4,5}, Patrick Nitchké⁶, Daniel Amram⁷, Marc-Lionel Bellaïche⁸, Veronique Abadie⁹, Marine Parodi¹⁰, Françoise Denoyelle¹⁰, Andrew Hattersley³, Christine Bole^{11,12}, Stanislas Lyonnet^{1,11,13} and Sandrine Marlin^{1,5,13}✉

© The Author(s), under exclusive licence to European Society of Human Genetics 2022

DNA polymerase δ is one of the three main enzymes responsible for DNA replication. *POLD1* heterozygous missense variants in the exonuclease domain result in a cancer predisposition phenotype. In contrast, heterozygous variants in *POLD1* polymerase domain have more recently been shown to be the underlying basis of the distinct autosomal dominant multisystem lipodystrophy disorder, MDPL (mandibular hypoplasia, deafness, progeroid features, and lipodystrophy syndrome OMIM # 615381), most commonly a recurrent in-frame deletion of serine at position 604, accounting for 18 of the 21 reported cases of this condition. One patient with an unusually severe phenotype has been reported, caused by a de novo c. 3209 T > A, (p.(Ile1070Asn)) variant in the highly conserved CysB motif in the C-terminal of the *POLD1* protein. This region has recently been shown to bind an iron-sulphur cluster of the 4Fe-4S type. This report concerns a novel de novo missense variant in the CysB region, c.3219 G > C, (p.(Ser1073Arg)) in a male child with a milder phenotype. Using in silico analysis in the context of the recently published structure of human Polymerase δ holoenzyme, we compared these and other variants which lie in close proximity but result in differing degrees of severity and varying features. We hypothesise that the c.3219 G > C, (p.(Ser1073Arg)) substitution likely causes reduced binding of the iron-sulphur cluster without significant disruption of protein structure, while the previously reported c.3209 T > A (p.(Ile1070Asn)) variant likely has a more profound impact on structure and folding in the region. Our analysis supports a central role for the CysB region in regulating *POLD1* activity in health and disease.

European Journal of Human Genetics (2022) 30:960–966; <https://doi.org/10.1038/s41431-022-01118-6>

INTRODUCTION

POLD1 encodes the catalytic subunit of DNA polymerase delta, which is responsible for lagging strand synthesis during DNA replication [1]. *POLD1* is also responsible for the critical proof-reading component of DNA replication, via a functionally distinct domain, the exonuclease domain. While pathogenic germline missense variants in the exonuclease domain of *POLD1* have long been known to result in predisposition to endometrial and colorectal cancer, de novo heterozygous variants in the polymerase domain have more recently been shown to be the underlying molecular basis for the distinct autosomal dominant multisystem lipodystrophy disorder, MDPL (mandibular hypoplasia, deafness, progeroid features, and lipodystrophy syndrome OMIM # 615381) [1]. This rare disorder is characterised by loss of subcutaneous fat, a characteristic facial appearance, metabolic disturbances, progressive sensorineural hearing loss and a milder longitudinal course than other progeroid disorders [1].

To date, there have been a total of 21 reported patients with MDPL caused by *POLD1* (NM_001256849.1) pathogenic variants, of which an in-frame deletion, c.1812_1814del, (p.(Ser605del)) in the polymerase active site is the most common, accounting for 18 of these cases [1–9]. Of the three patients harbouring other variants, 2 had de novo c.1572 C > T (p.(Arg507Cys)) substitutions [3, 8] and the third was the sole reported individual with a markedly severe progeroid phenotype, caused by a de novo c.3209 T > A (p.(Ile1070Asn)) variant located in the CysB motif [9]. This motif, spanning residues 1058–1076, lies in the extreme C-terminal region of *POLD1* and was previously thought to form a zinc finger. However, this has now been shown to bind an iron–sulphur cluster of the 4Fe-4S type, and this binding is crucial for efficient assembly and activity of the active DNA polymerase δ complex [10]. Figure 1 illustrates the architecture of the *POLD1* gene showing the relevant domains, the previously reported pathogenic variants in MDPL as well as the sequences of various *POLD1* orthologues around the CysB motif.

¹Service de Génétique Clinique, Hôpital Necker, Assistance Publique Hôpitaux de Paris (AP-HP), and Imagine Institute, 75015 Paris, France. ²Rosamund Stone Zander Translational Neuroscience Center, Boston Children's Hospital, Boston, USA. ³Institute of Biomedical and Clinical Science, University of Exeter School of Medicine, Exeter, UK. ⁴Service de Génétique Moléculaire, Hôpital Necker, AP-HP, Paris, France. ⁵Centre de Référence des Surdités Génétiques, Institut Imagine, Hôpital Necker, AP-HP, Paris, France. ⁶Bioinformatics Platform, Institut Imagine, Université Paris Descartes, Paris, France. ⁷Service de Génétique Clinique, Centre Hospitalier Intercommunal de Créteil, Créteil, France. ⁸Service de Gastroentérologie pédiatrique, Hôpital Robert Debré, AP-HP, Paris, France. ⁹Service de Pédiatrie, Hôpital Necker, AP-HP, Paris, France. ¹⁰Service d'ORL pédiatrique, Hôpital Necker, AP-HP, Paris, France. ¹¹Paris Descartes-Sorbonne Paris Cité Université, Institut Imagine, Paris, France. ¹²Genomics Platform, INSERM UMR 1163, Institut Imagine, Paris, France. ¹³INSERM-UMR1163, Institut Imagine, Paris, France. ✉email: sandrine.marlin@aphp.fr

Received: 11 March 2020 Revised: 21 May 2021 Accepted: 3 May 2022

Published online: 20 May 2022

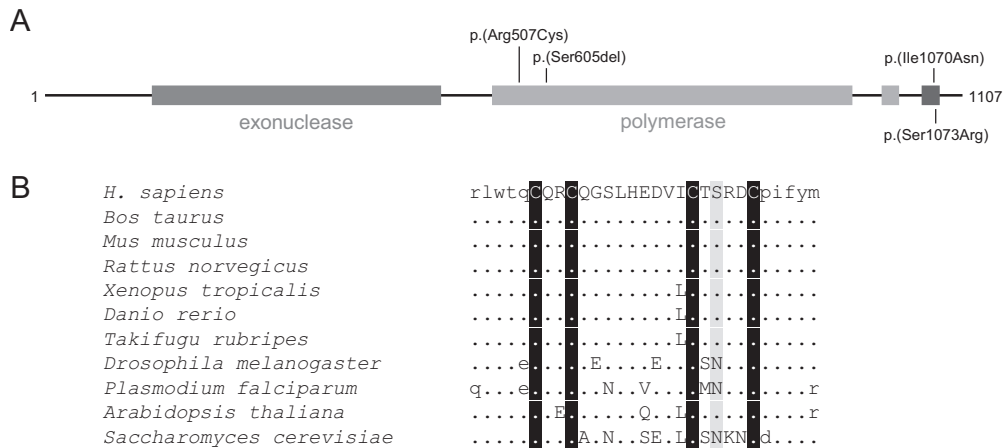


Fig. 1 Architecture of human DNA polymerase δ catalytic subunit and alignment of the CysB motif in *POLD1* orthologues. **A Schematic representation of the 1107 amino acid DNA polymerase δ catalytic subunit; right- and left-hatched boxes represent the conserved Pfam exonuclease (PF03104; residues 130-477) and polymerase (PF00136; residues 541-973) domains, respectively; open and filled boxes indicate the zinc-binding CysA motif (1012-1029) and the CysB iron-sulphur cluster (1058-1076), respectively; the position of previously-reported pathogenic variants in MDPL are shown above the schematic; the position of the novel p.(Ser1073Arg) variant is shown below. **B** The sequence of the human CysB motif (Cys1058-Cys1076) is shown in upper case, with flanking residues in lower case; the four cysteine residues of the iron-binding cluster are shown inverted, with Ser1073 shaded grey; the sequences of various *POLD1* orthologues are aligned below, with only differences to the human sequence shown.**

Here, we report a male patient presenting with growth delay, progressive hearing loss and mild progeroid features who was found by whole exome sequencing to harbour a different variant in the CysB domain of *POLD1*, namely c.3219 G > C, (p. (Ser1073-Arg)). He presented with the typically mild phenotype, in contrast to the severely affected patient with the c.3209 T > A (p. (Ile1070Asn)) variant. Using in silico analysis to compare these variants, we propose that the differences in observed phenotypes can be explained by differential changes in iron binding and active complex formation of the CysB domain.

SUBJECT AND METHODS

The subject, the third child of a healthy unrelated Caucasian parents with no family history of note, was referred for a genetics assessment for postnatal growth failure associated with microcephaly, progressive hearing loss and delayed development. The pregnancy was spontaneous and complicated by severe maternal hypertension. He was born at term with a birth weight of 3.3 kg (0 SD), length 48.5 cm (-1 SD) and a head circumference of 35 cm (0 SD).

Left cryptorchidism was noted on neonatal examination. He passed his neonatal hearing screen. He presented with feeding difficulties within the first few weeks of life. He started nocturnal enteral nutrition at the age of 3 years. Despite this, he had marked postnatal growth failure, with all growth parameters <-3.5 SDs.

With regard to his development, the patient started walking at 12 months. At 20 months, he presented with a delay in language acquisition and had a normal audiogram. At age 4 he had moderate bilateral sensorineural hearing loss, and by age 7, severe bilateral hearing loss. At age 8 there was progression in sign and oral language acquisitions but there was still a moderate intellectual disability.

On examination at age 5, weight was 11 kg (-3.5 SD), height 94 cm (-4 SD) and head circumference 46 cm (-5 SD). He had facial features suggestive of a disorder on the progeroid spectrum, with deeply set eyes, and a slightly pinched nose. He had low-set ears and small teeth (Fig. 2). His cardiorespiratory and gastrointestinal examinations were normal.

Brain MRI showed some mild enlargement of the lateral ventricles but was otherwise normal. CGH-array (60k) was normal. Metabolic investigations showed: normal phosphocalcic and

lipidic balances; growth hormone deficiency; normal thyroid and adrenal functions. Bone density was lower than normal ranges (Z score -4.9 for the whole body).

Whole exome sequencing (WES)

Trio whole exome sequencing was performed following informed consent. Exome capture was performed with the Agilent SureSelect Exome kit (58 Mb, V6) and sequenced on a HiSeq2500 (Illumina, Paris, France). Sequences were aligned to the reference human genome (GRCh37/hg19) using Burrows-Wheeler Aligner and variant calling was performed with HaplotypeCaller.

The mean depth of coverage obtained for each sample was >140x with more than 95% of the exome covered at least 30x. Variants were filtered against public SNP databases and more than 9000 in-house exomes from the Institut Imagine. We prioritised compound heterozygous, homozygous and maternally inherited X-linked variants with a frequency of <0.1% in public databases, and de novo variants with a frequency <0.01% in public databases.

Conservation analysis

Analysis of evolutionary conservation in *POLD1* was performed using the ConSurf server, as previously described [11].

Protein modelling and in silico analysis

All analysis was performed using the structure of the human DNA polymerase δ holoenzyme in complex with Proliferating cell nuclear antigen (PCNA) (PDB 6s1m; [12]). Amino acid substitutions were introduced and their effect on stability and protein-protein interactions analysed in silico using the FoldX modelling suite. In addition to the p.(Ser1073Arg) variant, we examined the effect of the previously reported p. (Ile1070Asn) variant and other reported variants in or near the CysB region. Physicochemical properties of the C-terminal region of native and variant *POLD1* sequences (residues 1001-1107) were analysed using the ExPASy ProtScale server.

RESULTS

Whole exome sequencing analysis

No plausible variants in disease genes corresponding to autosomal recessive and X-linked inheritance were identified. Three de novo heterozygous gene variants with a frequency of <0.01% were



Fig. 2 Facial features of index case, age 5 years. Facial features on the progeroid spectrum with deeply set eyes and a pinched nose.

identified, of which the only plausible candidate was a missense variant in *POLD1* NM_001256849.1, c.3219 C > G; this affects the first nucleotide of the final exon (exon 27 of NM_001256849.1) and is predicted to lead to substitution of serine for arginine at position 1073. The details of all rare de novo variants are shown in Table S1. This variant was absent in public databases (gnomAD, dbSNP, ClinVar, HGMD) and on the in-house database of >9000 exomes. It was predicted to be pathogenic on Polyphen-2 and deleterious on Mutation Taster and CADD but benign on SIFT. The presence of the variant was confirmed on direct gene sequencing. The variant was submitted to ClinVar (SUB9578857).

Using the suite of prediction tools available via Alamut Visual v2.10 (Interactive Biosoftware, Rouen, France), a modest increase in the efficiency of the exon 27 splice acceptor was predicted, suggesting that altered splicing was unlikely to have a significant effect on *POLD1* expression.

Conservation analysis

While nucleotide c.3219 is not conserved, serine is present at this position in all vertebrates where *POLD1* orthologues have been identified and annotated. The c.3219 C > G, (p.(Ser1073Arg)) variant has not been reported in the gnomAD database; a different variant affecting the same codon, c.3217 A > G, (p.(Ser1073Gly)), has been reported as a heterozygous variant in a single individual.

Analysis of evolutionary conservation using ConSurf showed that the CysB region (residues 1058–1076) is highly conserved, with an average ConSurf grade of 8.16 out of 9 over this region. In the multiple sequence alignment compiled by ConSurf, serine was present at position 1073 in 74.83% of sequences, with the only other amino acids represented being asparagine (23.78%) and alanine (1.40%). The four cysteine residues at positions 1058, 1061, 1071 and 1076, which bind the 4Fe-4S cluster, were invariant in all sequences.

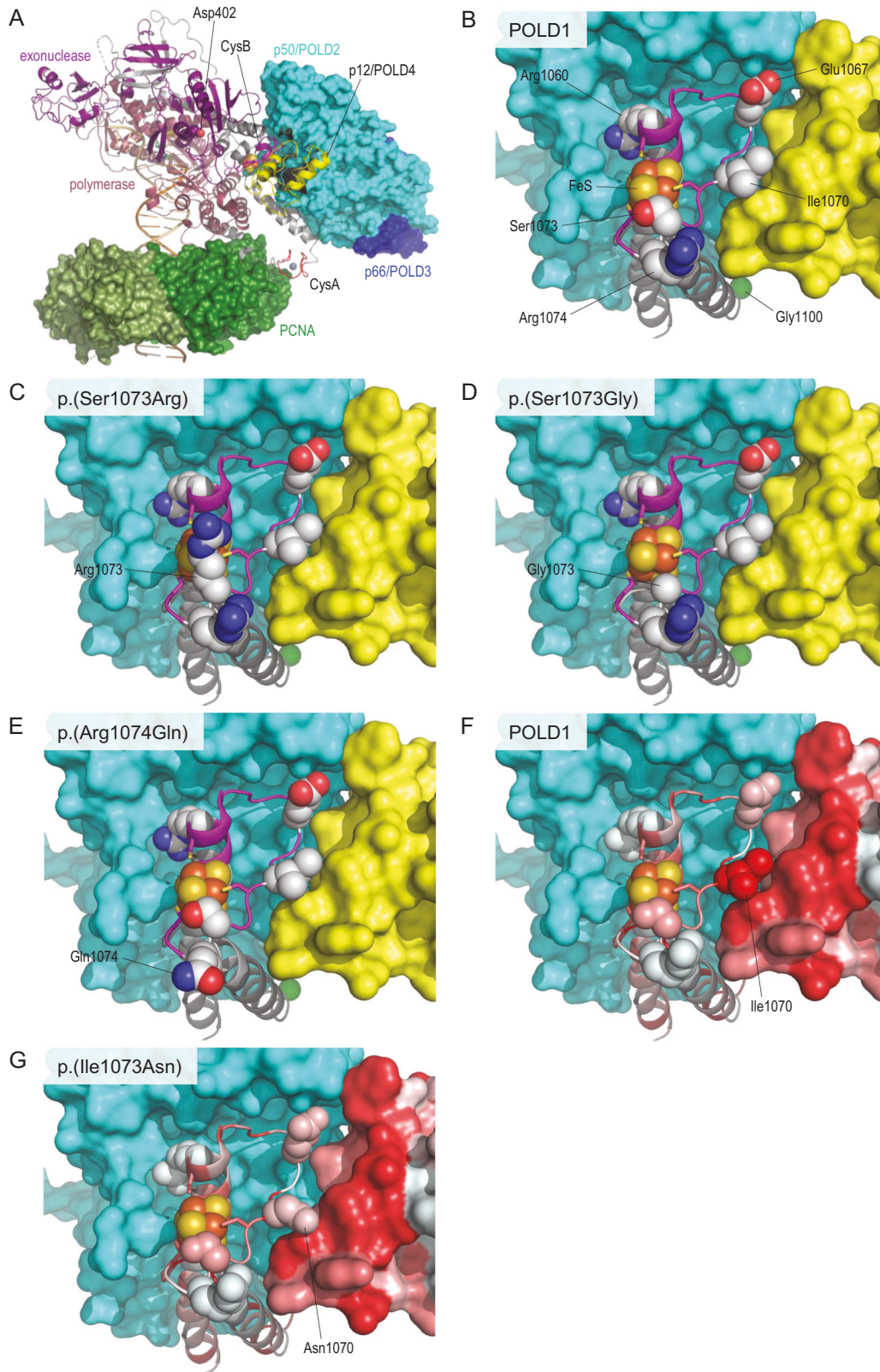
Protein modelling

Structures for the human Polymerase δ holoenzyme in complex with PCNA have recently been reported. These show that while the CysA region of *POLD1* interacts with PCNA, the CysB region lies at the core of the holoenzyme, making interactions with the p50/*POLD2* and p12/*POLD4* subunits of the holoenzyme, as well as intramolecular interactions with other regions of *POLD1* (Fig. 3A). The iron-sulphur cluster itself lies within a deep pocket, coordinated by four conserved cysteine residues (Cys1058, 1061,

1071 and 1076; Fig. 3B), suggesting that the cluster acts as a nucleus for folding of the region.

The p.(Ser1073Arg) variant introduced the large, charged side-chain of arginine in place of the small, uncharged polar sidechain of serine. This residue is accessible at the surface of the cluster binding pocket, and the variant did not appear to result in any steric clashes at the atomic level which might directly affect protein stability (Fig. 3C). However, the presence of the positively charged sidechain close to the cluster binding site is likely to reduce binding of the positively charged [4Fe-4S]²⁺ cluster as a result of electrostatic clashes. For comparison, we analysed the p.(Ser1073Gly) and p.(Arg1074Gln) substitutions, both of which have been observed as heterozygous variants in the gnomAD database with one and four counts, respectively, and are thus presumed to be benign. Neither variant was predicted to cause an obvious structural defect (Fig. 3D, E), with the sidechain of residue 1074 pointing away from the CysB cluster binding pocket. Substitution of p.Ile1070 by asparagine has been reported to cause a more severe MDPL phenotype. This residue lies in direct contact with p.Trp102 and p.Leu107 of the p12/*POLD4* subunit, and is directly adjacent to one of the conserved cysteine residues (Fig. 3F). Substitution by the polar asparagine group was predicted to destabilise the structure of the CysB region, probably as a result of the large difference in polarity between the native and variant sidechains, as well as weakening the interaction with p12/*POLD4* as a result of altered hydrophobicity (Fig. 3G). The FoldX modeling suite does not alter the position of the protein backbone when creating amino acid substitutions, hence in our model the path of the CysB loop appeared unaffected. However, in vivo it is likely that the large change in polarity and hydrophobicity caused by the p.(Ile1070Asn) variant (Fig. 4) results in altered topology of the loop, such that the position of the cluster-binding residue Cys1071 is altered. Conversely, the effect of the p.(Ser1073Arg) variant on these properties was modest, while the two gnomAD variants, p.(Ser1073Gly) and p.(Arg1074Gln), had no significant effect on polarity or hydrophobicity in this region.

In addition to the above variants, other missense substitutions have been reported in and around the CysB region, namely p.(Arg1060Cys) [13], p.(Glu1067Lys) [14] and p.(Gly1100Arg) [15], the latter of which lies C-terminal of the core CysB region. Interestingly, while the heterozygous p.(Glu1067Lys) variant was reported in a case of partial lipodystrophy, p.(Arg1060Cys) was observed as a homozygous variant in a patient presenting with lymphopenia and sensorineural hearing loss, and the



p.(Gly1100Arg) variant was present as a compound heterozygote along with a presumed loss of function variant (p.Ser197Hisfs*54) in a patient with non-syndromic hearing loss. While sensorineural hearing loss is a feature of MDPL syndrome, there is considerable variability in the other features presented in these cases. We

performed modelling on these variants to assess whether there were differences in their molecular effects. All variants had unique and subtly different effects on POLD1 and its interactions with other subunits of the Polymerase δ holoenzyme (details shown in Fig. S1A–E and Table S2), suggesting a molecular basis for

Fig. 3 Structure of POLD1 and CysB variants. A Structure of the Polymerase δ holoenzyme in complex with PCNA (PDB 6s1m; Lancey et al., 2020). The p125/POLD1 subunit is shown in ribbon format; polymerase and exonuclease domains are coloured raspberry and purple respectively, while CysA and CysB regions are red and magenta. Surfaces are shown for p50/POLD2 (cyan), p66/POLD3 (blue) and PCNA (shades of green); the p12/POLD4 subunit is shown as a yellow ribbon. **B** Detail around the bound iron-sulphur cluster (FeS) in the CysB region; sidechains are shown in stick format for the four conserved cysteine residues, and as space-filling spheres for other residues of interest as labelled. For clarity, only residues 1000–1107 of POLD1 are shown. Surfaces are shown for p50/POLD2 (cyan) and p12/POLD4 (yellow). **C–E** As **(B)**, but showing predicted structures of the variants p.(Ser1073Arg), p.(Ser1073Gly) and p.(Arg1074Gln), respectively. **F** As **(B)**, but showing p125/POLD1 and p12/POLD4 coloured by hydrophobicity (red, most hydrophobic to white, most polar). **G** As **(F)** but showing predicted structure for the p.(Ile1070Asn) variant.

the range of phenotypes seen in association with different variants in CysB. Finally, we also examined the context of the previously-reported variant Arg507Cys, observed in a case of MDPL [3]. While this residue lies outside the annotated functional domains of POLD1, its sidechain is directed towards the CysB region where it forms a hydrogen bond to the backbone of p.Asp1068; this bond was absent in the variant, thereby removing a molecular connection between CysB and other regions of POLD1 (Fig. S1F–G)

DISCUSSION

We report a further patient with MDPL syndrome caused by a novel *de novo* pathogenic *POLD1* variant c.3219G>C (p.(Ser1073Arg)). In a recent review of 21 affected patients, mandibular hypoplasia, progeroid features and lack of subcutaneous fat emerged as the most consistent clinical features [16]. While the presence of hearing impairment in combination with these features is highly suggestive of MDPL, the onset of hearing loss is variable and several adult patients with normal hearing have been reported [16].

Long-term natural history data for MDPL is lacking but timely diagnosis enables surveillance for a range of potential metabolic complications, including impaired glucose intolerance, dyslipidaemia, elevated total cholesterol, hepatic steatosis and osteoporosis [1, 16]. Male hypogonadism is common, as is menstrual disturbance in female patients. Our patient demonstrated growth hormone deficiency, and is currently undergoing evaluation for rhGH treatment, which has been used for two other patients [16]. Overall, the disorder is considered to be on the mild end of the progeria spectrum, with no evidence of accelerated atherosclerotic disease or premature death, the only exception being the severely affected patient with the c.3209T>A (p.(Ile1070Asn)) variant [9]. Our patient presented with a degree of developmental delay which cannot be solely explained by his hearing loss. While most patients with MDPL are reported as cognitively normal, we suspect that developmental delay may be an under-reported feature of MDPL. Indeed, *POLD1* has been recently implicated in cognitive development in a mouse model [17]. We cannot, however, rule out the possibility that the neurodevelopmental difficulties are unrelated to the *POLD1* variant in our patient.

Molecular modeling of p.(Ser1073Arg) and other previously reported pathogenic variants in and around the CysB region showed that all variants appeared to have subtly different effects on POLD1, with some also predicted to affect interactions with other components of the Polymerase δ holoenzyme. Specifically, the p.(Ser1073Arg) variant was predicted to have a relatively minor effect on binding of the iron-sulphur cluster due to electrostatic repulsion, while p.(Ile1070Asn) likely had a more profound effect on the structure of cluster binding pocket, while also affecting interactions with p50/POLD2. We hypothesise that the severity of these molecular effects reflects the observed difference in phenotypes of patients carrying these variants.

A recent functional study of the CysB region has shown that different variants within this region have different outcomes on the structure and activity of the Polymerase δ holoenzyme [18]. Specifically, substitution of p.Cys1076, one of the four cluster-binding cysteine residues, to serine, resulted in a ~10-fold

decrease in iron binding; however, in contrast to studies on POL3, the yeast orthologue of POLD1, this variant was able to assemble into a holoenzyme complex, albeit with greatly reduced thermal stability compared to wild-type. This stability could be rescued by the presence of PCNA, which also restored the strong defect in polymerase activity as measured in a primer extension reaction. However, the variant also showed a defect in exonuclease activity which was not rescued by PCNA. By comparison, tyrosine or tryptophan substitution of His1066 caused only a small to moderate loss of iron binding (20% and 50% respectively), and the variants assembled normally into holoenzyme with wild-type polymerase activity. Both variants exhibited a similar defect in exonuclease activity to that observed for the p.(Cys1076Ser) variant. This demonstrates not only that the structure of the CysB region is crucial for the activity of POLD1, but that changes in this structure can be sensed and transmitted to the catalytic centres of both the polymerase and exonuclease domains. In this respect it is intriguing that p.Arg507, the site of a reported missense variant in MDPL, makes direct contact with the CysB region and thus may form part of that sensing mechanism. The different molecular effects observed for substitutions at p.Cys1076 and p.His1066 give also rise to the potential for different outcomes in cellular development. Molecular modeling suggests that different variants in and around the CysB region will have different effects on binding and/or accessibility of the iron-sulphur complex, and interactions with other components of the holoenzyme, potentially resulting in subtle differences in enzyme activity which in turn lead to the different phenotypes observed. However, in the case of MDPL, it is not yet understood how the molecular defect in DNA polymerase δ activity results in disease, or what cell type(s) may be affected. One possibility is that a partial defect in DNA replication renders cells more prone to apoptosis under proliferative conditions, and that in MDPL this specifically affects preadipocytes during proliferation and differentiation accompanying adipose tissue development. Conversely, the p.(Arg1060Cys) substitution, which alters the interaction between POLD1 and POLD2/p50, was shown to specifically affect the expansion of peripheral CD8⁺ T-cells [13]. Thus the phenotype observed presumably reflects the different sensitivity of various cell types to the specific molecular defect resulting from the variant.

The *POLD1* gene is tolerant to monoallelic loss of function in the human population, with a gnomAD pLI score (probability that the gene is intolerant to loss of function) of 0 and an observed/expected LoF score of 0.36 (90% CI 0.25–0.53). The z score for constraint against missense variation is 2.46 (with a higher z score reflecting intolerance to missense variation, a score of >3.09 being considered with excessively constrained) [19]. It is most likely that MDPL is due to pathogenic missense variants in *POLD1* which result in gain-of-function or a dominant negative effect. In the case of variants in the CysB region, the potential for a dominant negative effect is revealed by the work of Jozwiakowski et al. [18], who showed that variants which disrupted binding of the iron-sulphur cluster retained the ability to interact with other subunits of Polymerase δ . In contrast, Oh et al. [15] reported that the p.(Ile1070Asn) variant was unable to interact with other subunits. It is possible that this discrepancy was due to technical differences in the methods used, as Oh et al. attempted to reconstitute

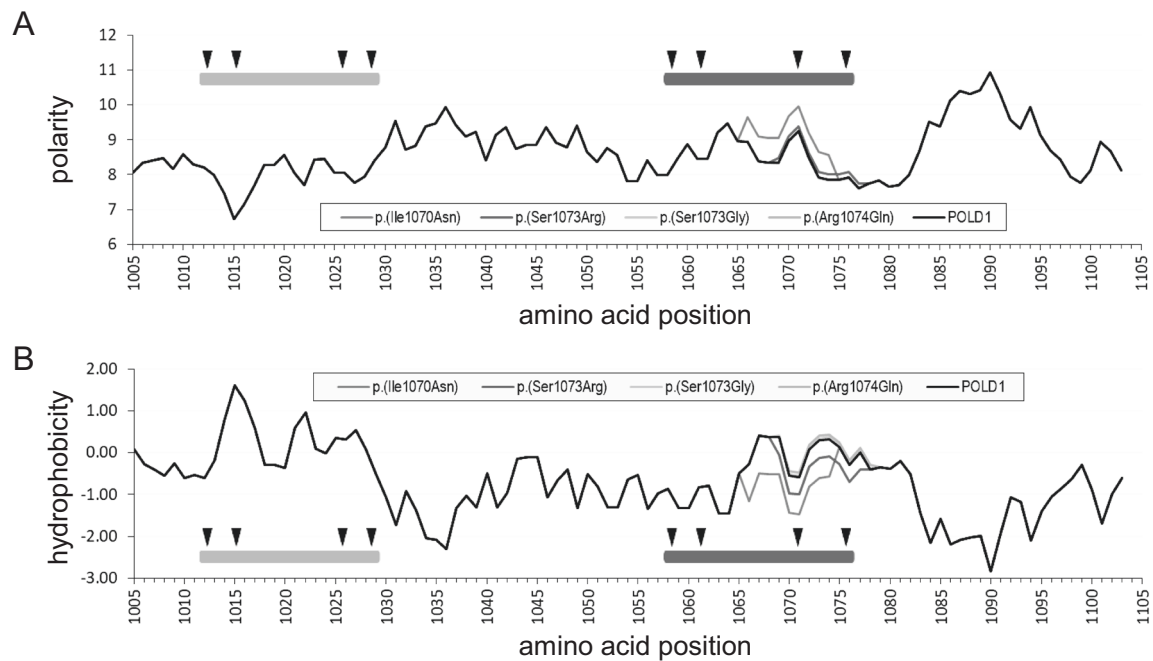


Fig. 4 Physicochemical properties of the CysA and CysB regions of POLD1. **A** Polarity (Grantham scale) of the C-terminal of POLD1 (residues 1001-1107), calculated in 9-residue windows; data are plotted for wild-type POLD1 and missense variants as shown. **B** As (**A**), but showing data for amino acid hydrophobicity (Kyte-Doolittle scale). In both parts, open or filled bars indicate the extent of the CysA or CysB motifs respectively, with black arrows indicating positions of conserved cysteine residues.

Polymerase δ holoenzyme in vitro from individually purified recombinant proteins, whereas Jozwiakowski et al. performed a one-step affinity purification of the intact complex from *Sf9* insect cells co-expressing all holoenzyme subunits. Therefore, while it is possible that the p.(Ile1070Asn) variant is in some other way able to affect or interfere with the normal activity of the holoenzyme, it seems likely that this and other pathogenic CysB variants exert their dominant activity by retaining the ability to be incorporated into holoenzyme complexes of reduced or altered activity. We have not performed physical or functional characterisation of the POLD1 p.(Ser1073Arg) variant protein, although as the variant occurs in a heterozygous state, we assume the protein retains the ability to interact with other components of the holoenzyme complex and thus exerts a gain-of-function or dominant negative effect. Indeed, given the apparent sensitivity of results from in vitro assays to aspects of the experimental design, it may be more constructive to focus future research efforts on first identifying the relevant cell type(s) affected by MDPL-associated variants, followed by characterisation of the precise defect in DNA polymerase δ activity in the cellular context.

Recently, a large number of *POLD1* variants were identified in a cohort of patients with various dyslipidemias [20]. The majority of the variants (59/72) have also been reported in gnomAD v2.1.1, and range from the very rare (carrier frequency, 1/126,000 individuals) to the very common (carrier frequency, 1/4). While the presence of some of these may be unrelated, it is possible that hypomorphic variants or functional polymorphisms in *POLD1* may confer a polygenic risk to various forms of lipidemia. Notably however, none of the patients in the cohort was reported as having the MDPL phenotype; moreover, neither the previously-reported variants in MDPL (p.(Arg507Cys), p.(Ser605del), p.(Ile1070Asn)) nor the novel p.(Ser1073Arg) variant were observed, and in fact no variants in the CysB motif were reported in the cohort. This is consistent with the hypothesis that MDPL is a distinct Mendelian disorder caused by rare variants which have a more profound effect on the function of POLD1.

In summary, we report a male patient presenting with typical MDPL caused by a de novo novel variant in the CysB domain of *POLD1*. Our patient presented with the typically mild phenotype, in contrast to the severely affected patient with the p.(Ile1070Asn) variant. Using in silico comparison of these and other variants, we propose that the differences in observed phenotype can be explained by differential changes in the structure of the CysB region, its interactions with other subunits of the Polymerase δ holoenzyme and the balance between the different catalytic activities of this complex. Thus, while detailed analysis is still required to confirm the effects of p.(Ser1073Arg) variant, this work highlights the central role of the CysB region in coordinating the various activities of the Polymerase δ holoenzyme.

Web Resources

- gnomAD browser, <http://gnomad.broadinstitute.org/>
- OMIM, <http://www.omim.org/>
- PolyPhen-2 v.2.2.2, <http://genetics.bwh.harvard.edu/pph2/>
- SIFT v.1.03, <http://sift.bii.a-star.edu.sg/>
- ExPASy ProtScale, <https://web.expasy.org/protscale/>
- <http://foldxsuite.crg.eu/>

DATA AVAILABILITY

The variant identified in this project has been submitted to a publicly accessible genetic variant database, ClinVar. The ClinVar accession number is SUB9578857.

REFERENCES

1. Weedon MN, Ellard S, Prindle MJ, Caswell R, Allen HL, Oram R, et al. An in-frame deletion at the polymerase active site of POLD1 causes a multisystem disorder with lipodystrophy. *Nat Genet.* 2013;45:947–50.
2. Shastri S, Simha V, Godbole K, Sbraccia P, Melancon S, Yajnik CS, et al. A Novel Syndrome of Mandibular Hypoplasia, Deafness, and Progeroid Features

- Associated with Lipodystrophy, Undescended Testes, and Male Hypogonadism. *J Clin Endocrinol Metab.* 2010;95:E192–7.
3. Pelosini C, Martinelli S, Ceccarini G, Magno S, Barone I, Basolo A, et al. Identification of a novel mutation in the polymerase delta 1 (POLD1) gene in a lipodystrophic patient affected by mandibular hypoplasia, deafness, progeroid features (MDPL) syndrome. *Metab Clin Exp.* 2014;63:1385–9.
 4. Fiorillo C, D'Apice MR, Trucco F, Murdocca M, Spitalieri P, Assereto S, et al. Characterization of MDPL Fibroblasts Carrying the Recurrent p.Ser605del Mutation in *POLD1* Gene. *DNA Cell Biol.* 2018;37:1061–7.
 5. Okada A, Kohmoto T, Naruto T, Yokota I, Kotani Y, Shimada A, et al. The first Japanese patient with mandibular hypoplasia, deafness, progeroid features and lipodystrophy diagnosed via *POLD1* mutation detection. *Human Genome Variation [Internet].* 2017[cited 2019 May 28];4. <http://www.nature.com/articles/hgv201731>
 6. Wang LR, Radonjic A, Dillio AA, McIntyre AD, Hegele RA. A De Novo *POLD1* Mutation Associated With Mandibular Hypoplasia, Deafness, Progeroid Features, and Lipodystrophy Syndrome in a Family With Werner Syndrome. *J Investig Med High Impact Case Rep.* 2018;6:232470961878677.
 7. Reinier F, Zoledziewska M, Hanna D, Smith JD, Valentini M, Zara I, et al. Mandibular hypoplasia, deafness, progeroid features and lipodystrophy (MDPL) syndrome in the context of inherited lipodystrophies. *Metab Clin Exp.* 2015;64:1530–40.
 8. Lessel D, Hisama FM, Szakson K, Saha B, Sanjuanelo AB, Salbert BA, et al. *POLD1* Germline Mutations in Patients Initially Diagnosed with Werner Syndrome. *Hum Mutat.* 2015;36:1070–9.
 9. Elouej S, Belezza-Meireles A, Caswell R, Colclough K, Ellard S, Desvignes JP, et al. Exome sequencing reveals a de novo *POLD1* mutation causing phenotypic variability in mandibular hypoplasia, deafness, progeroid features, and lipodystrophy syndrome (MDPL). *Metabolism* 2017;71:213–25.
 10. Netz DJA, Pierik AJ, Stümpfig M, Bill E, Sharma AK, Pallesen LJ, et al. A Bridging [4Fe–4S] Cluster and Nucleotide Binding Are Essential for Function of the Cfd1-Nbp35 Complex as a Scaffold in Iron-Sulfur Protein Maturation. *J Biol Chem.* 2012;287:12365–78.
 11. Ashkenazy H, Abadi S, Martz E, Chay O, Mayrose I, Pupko T, et al. ConSurf 2016: an improved methodology to estimate and visualize evolutionary conservation in macromolecules. *Nucleic Acids Res.* 2016;44:W344–350. 08
 12. Lancey C, Tehseen M, Raducanu V-S, Rashid F, Merino N, Ragan TJ, et al. Structure of the processive human Pol δ holoenzyme. *Nat Commun.* 2020;11:1109. 28
 13. Cui Y, Keles S, Charbonnier L-M, Julé AM, Henderson L, Celik SC, et al. Combined immunodeficiency caused by a loss-of-function mutation in DNA polymerase delta 1. *J Allergy Clin Immunol.* 2020;145:391–401.e8.
 14. Ajluni N, Meral R, Neidert AH, Brady GF, Buras E, McKenna B, et al. Spectrum of disease associated with partial lipodystrophy: lessons from a trial cohort. *Clin Endocrinol.* 2017;86:698–707.
 15. Oh D-Y, Matsumoto Y, Kitajiri S-I, Kim NKD, Kim MY, Kim AR, et al. *POLD1* variants leading to reduced polymerase activity can cause hearing loss without syndromic features. *Hum Mutat.* 2020;41:913–20.
 16. Sasaki H, Yanagi K, Ugi S, Kobayashi K, Ohkubo K, Tajiri Y, et al. Definitive diagnosis of mandibular hypoplasia, deafness, progeroid features and lipodystrophy (MDPL) syndrome caused by a recurrent *de novo* mutation in the *POLD1* gene. *Endocr J.* 2017;65:227–38.
 17. Gao S, Zhang X, Song Q, Liu J, Ji X, Wang P. *POLD1* deficiency is involved in cognitive function impairment in AD patients and SAMP8 mice. *Biomed Pharmacother.* 2019;114:108833.
 18. Jozwiakowski SK, Kummer S, Gari K. Human DNA polymerase delta requires an iron–sulfur cluster for high-fidelity DNA synthesis. *Life Sci Alliance.* 2019;2:e201900321.
 19. Samocha KE, Robinson EB, Sanders SJ, Stevens C, Sabo A, McGrath LM, et al. A framework for the interpretation of *de novo* mutation in human disease. *Nat Genet.* 2014;46:944–50.
 20. Dron JS, Wang J, McIntyre AD, Iacocca MA, Robinson JF, Ban MR, et al. Six years' experience with LipidSeq: clinical and research learnings from a hybrid, targeted sequencing panel for dyslipidemias. *BMC Med Genom.* 2020;13:23.

ACKNOWLEDGEMENTS

The authors of this paper wish to acknowledge the patient and family for their participation in this study. The authors would also like to thank Andrew Hattersley for his critical review of the paper. The authors of this paper wish to acknowledge the Fondation Bettencourt-Schueller, MSD-France and the patient organization “S’entendre” for their financial supports.

COMPETING INTERESTS

The authors declare no competing interests.

ETHICS APPROVAL

IRB approval was not required for this case report, as per French regulatory guidelines. Informed consent was obtained for the publication of photographs.

ADDITIONAL INFORMATION

Supplementary information The online version contains supplementary material available at <https://doi.org/10.1038/s41431-022-01118-6>.

Correspondence and requests for materials should be addressed to Sandrine Marlin.

Reprints and permission information is available at <http://www.nature.com/reprints>

Publisher's note Springer Nature remains neutral with regard to jurisdictional claims in published maps and institutional affiliations.